© 2024. Published by The Company of Biologists Ltd | Development (2024) 151, dev202586. doi:10.1242/dev.202586

RESEARCH ARTICLE

HD-Zip II transcription factors control distal stem cell fate in *Arabidopsis* roots by linking auxin signaling to the FEZ/SOMBRERO pathway

Marco Possenti[1,*], Giovanna Sessa[2,*], Altea Alfè[2], Luana Turchi[2], Valentino Ruzza[2], Massimiliano Sassi[2,¶], Giorgio Morelli[1,‡,¶] and Ida Ruberti[2,‡,§]

ABSTRACT

In multicellular organisms, specialized tissues are generated by specific populations of stem cells through cycles of asymmetric cell divisions, where one daughter undergoes differentiation and the other maintains proliferative properties. In *Arabidopsis thaliana* roots, the columella – a gravity-sensing tissue that protects and defines the position of the stem cell niche – represents a typical example of a tissue whose organization is exclusively determined by the balance between proliferation and differentiation. The columella derives from a single layer of stem cells through a binary cell fate switch that is precisely controlled by multiple, independent regulatory inputs. Here, we show that the HD-Zip II transcription factors (TFs) HAT3, ATHB4 and AHTB2 redundantly regulate columella stem cell fate and patterning in the *Arabidopsis* root. The HD-Zip II TFs promote columella stem cell proliferation by acting as effectors of the FEZ/SMB circuit and, at the same time, by interfering with auxin signaling to counteract hormone-induced differentiation. Overall, our work shows that HD-Zip II TFs connect two opposing parallel inputs to fine-tune the balance between proliferation and differentiation in columella stem cells.

KEY WORDS: HD-Zip II, Stem cells, Auxin, Proliferation, Root development, Columella

INTRODUCTION

The balance between stemness and differentiation, which is key for the generation of specialized tissues in multicellular organisms, is governed by asymmetric cell divisions (ACDs). When a cell divides asymmetrically, it generates two daughter cells with different fates: one retains the self-renewal properties of the mother, whereas the other acquires a specific cell fate and is committed to differentiate (Pierre-Jerome et al., 2018; Pillitteri et al., 2016). In plants, where the presence of a cell wall limits the movement of cells within the tissues, the coordination between cell proliferation and differentiation in the shoot and root apical meristem (SAM and RAM, respectively) is essential to ensure proper developmental processes throughout the lifespan of the plant (De Smet and Beeckman, 2011).

Because of its stereotypical organization, the RAM of *Arabidopsis thaliana* represents an ideal system in which to study the coordination between proliferation and differentiation in plant development. The stem cell niche (SCN) in the *Arabidopsis* RAM is centered around a group of slowly replicating cells, the quiescent center (QC), which functions as stem cell organizer (Scheres, 2007). The QC is surrounded by two different pools of stem cells (also known as initials) that produce daughters that give rise to all the tissues of the root (Dolan et al., 1993; Scheres, 2007). The daughters located at the proximal and lateral sides of the QC form a transit-amplifying population (the proximal RAM) that undergoes several rounds of divisions before differentiating into specialized cells. By contrast, the daughters of columella stem cells (CSCs), which are located distal to the QC, directly differentiate into columella cells (CCs) and accumulate starch granules in amyloplasts for gravity sensing (Scheres, 2007). Because CC ultimately detach from the root cap, the coordination of CSC proliferation and daughter cell differentiation must be tightly controlled to maintain a constant number of CC tiers, and thus a correct positioning of the SCN within the RAM (Scheres, 2007).

A number of independent yet intertwined pathways regulate the maintenance of distal stem cells by controlling the activity of the QC, the proliferation of CSC and the differentiation of daughter cells (Pardal and Heidstra, 2021; Shimotohno and Scheres, 2019). The homeobox gene *WUSCHEL-RELATED HOMEOBOX 5* (*WOX5*), has a central role in regulation of distal stem cells. WOX5 is expressed in the QC, where it acts cell-autonomously to suppress cell divisions by excluding CYCLIN D3;3 activity from the QC (Forzani et al., 2014). On the other hand, WOX5 suppresses the differentiation of CSC non-cell-autonomously by repressing the expression of *CYCLING DOF FACTOR 4* (*CDF4*) via chromatin modifications upon interaction with TOPLESS (TPL) co-repressor (Pi et al., 2015). The control of QC activity and CSC maintenance by WOX5 also depends on cross-regulation and physical interactions with members of the PLETHORA (PLT) family of transcription factors (TFs) (Burkart et al., 2022). As a result, *wox5* mutants display differentiated CSCs but enhanced QC division to replenish shedding columella tiers, whereas WOX5 overexpression causes CC dedifferentiation (Bennett et al., 2014; Forzani et al., 2014; Sarkar et al., 2007).

Auxin also plays a crucial role in the maintenance of distal stem cells through the formation of an instructive hormone gradient spanning from the QC throughout the CC (Ding and Friml, 2010; Dubreuil et al., 2018; Sabatini et al., 1999). The auxin gradient is generated and maintained through a combination of local hormone

[1]Research Centre for Genomics and Bioinformatics, Council for Agricultural Research and Economics (CREA), Rome 00178, Italy. [2]Institute of Molecular Biology and Pathology, National Research Council, Rome 00185, Italy.
*These authors contributed equally to this work ‡These authors jointly supervised this work §Deceased

¶Authors for correspondence (massimiliano.sassi@cnr.it; giorgio.morelli.crea@gmail.com)

M.P., 0000-0001-6707-3245; G.S., 0000-0003-0093-3495; M.S., 0000-0002-9685-4902; G.M., 0000-0002-8994-4838

Handling Editor: Dominique Bergmann
Received 6 December 2023; Accepted 20 March 2024

Development (2024) 151, dev202586. doi:10.1242/dev.202586

biosynthesis in the QC and polar transport within the distal tissues (Blilou et al., 2005; Stepanova et al., 2008). Interestingly, auxin biosynthesis in the QC is regulated by the action of WOX5 and, in turn, high auxin levels promote CSC differentiation at least in part by downregulating *WOX5* expression (Ding and Friml, 2010; Savina et al., 2020; Tian et al., 2014). Auxin-mediated WOX5 downregulation has been linked to the AUXIN RESPONSE FACTOR (ARF) 10 and ARF16 transcriptional regulators, which also play a role in restricting the SCN and promoting CC differentiation (Ding and Friml, 2010; Wang et al., 2005). Double *arf10 arf16* mutants, or plants overexpressing *MIR160* – a microRNA that downregulates *ARF10* and *ARF16* – display uncontrolled cell division and blocked cell differentiation in distal root tissues (Wang et al., 2005). Whether ARF10 and ARF16 are required for the auxin-mediated downregulation of WOX5 is still not clear, and it has been proposed that the two pathways act in parallel to regulate distal stem cell activity (Bennett et al., 2014).

Other than the auxin/WOX5 pathways, NAC transcription factors FEZ and SOMBRERO (SMB) are intrinsically required for correct developmental program of distal tissues (Bennett et al., 2014; Willemsen et al., 2008). Both *fez* and *smb* loss-of-function mutants display alterations in the number of columella and lateral root cap (LRC) cell layers from embryogenesis onward (Willemsen et al., 2008). In particular, *fez* mutants show a reduction in the number of columella and LRC layers due to lower frequency of CSC and epidermis (Epi)/LRC initial divisions, whereas *smb* mutants display additional CSC and LRC layers as a consequence of delayed differentiation (Willemsen et al., 2008). It has been proposed that FEZ and SMB operate in a self-regulatory loop to control CSC proliferation: FEZ is expressed in CSCs, where it induces ACD but is repressed by SMB in apical daughters to prevent further division and promote CC differentiation (Willemsen et al., 2008). Remarkably, this regulatory loop interacts with the WOX5 pathway, as it has been shown that WOX5 cell-autonomously represses FEZ expression in the QC to maintain quiescence, and non-cell-autonomously represses *SMB* in CSCs to prevent differentiation (Bennett et al., 2014). Together, these studies clearly depict that distal stem cell activity does not rely on unified pathways regulating either proliferation or differentiation, but it rather depends on the convergence of multiple quantitative inputs, with presumably additional factors mediating regulatory interactions between known players (Bennett et al., 2014).

Here, we identify members of the HD-Zip II TF family as additional regulators of distal stem cell activity in roots. We show that developmental regulators HOMEOBOX ARABIDOPSIS THALIANA 3 (HAT3), ARABIDOPSIS THALIANA HOMEOBOX 4 (ATHB4) and ATHB2, which are known for their role in the control of apical embryo patterning and shoot architecture (Carabelli et al., 2021; Merelo et al., 2016; Turchi et al., 2013), redundantly regulate distal stem cell activity and columella organization. We provide evidence that HD-Zip II proteins regulate CSC activity by interfering locally with auxin signaling and, at the same time, by acting downstream of FEZ. Our work shows that HD-Zip II proteins control the balance between CSC proliferation and CC differentiation by bridging the gap between the FEZ/SMB and auxin pathways.

RESULTS

Simultaneous mutations of *HAT3*, *ATHB4* and *ATHB2* affect RAM size and patterning

Previous work has demonstrated that HAT3, ATHB4 and ATHB2 act redundantly in the regulation of shoot architecture (Carabelli et al., 2021; Merelo et al., 2016; Turchi et al., 2013); therefore, we wondered whether these TFs also play a role in root development. To this end, we characterized root phenotypes of single and double HD-Zip II mutant combinations. The root length and RAM size of *hat3-3 athb4-1* mutant seedlings were slightly, although significantly, reduced compared with the wild type (Fig. S1). Similar defects were observed in different allelic combinations (*hat3-3 athb4-3* and *hat3-2 athb4-1*) and were fully rescued by introgressing an *HAT3::HAT3:GFP* construct in *hat3-3 athb4-1* (Fig. S1). Single mutant analyses revealed that only *hat3-3* displays reduced root length and RAM size as *hat3 athb4*, suggesting that these phenotypes are not determined by the altered shoot development of the double mutant (Fig. S1; Turchi et al., 2013). Closer inspection of *hat3-3 athb4-1* seedlings revealed defects in root tip organization. Irregular division patterns and abnormal QC and CC shapes were observed in more than 75% of the *hat3-3 athb4-1* root tips (Table S1) and at a similar level in other allelic combinations. Root tip organization defects were only partially rescued by expressing *HAT3::HAT3:GFP* in *hat3-3 athb4-1* (Table S1). No significant alteration in the root tip organization of single mutants was observed (Table S1), indicating that HAT3 and ATHB4 function redundantly in this process. Next, we investigated whether lack of ATHB2 aggravates the *hat3 athb4* phenotype. Different allelic combinations of the *hat3 athb4 athb2* triple mutants displayed an increased severity of the root phenotypes observed in *hat3 athb4*. Reductions in root length and RAM size in *hat3 athb4 athb2* were already visible in 5-day-old seedlings, further reaching a dramatic decrease in 10-day-old plantlets (Fig. 1C,D, Fig. S1); defects in QC/CC patterning were observed at a higher frequency in *hat3 athb4 athb2* compared with double mutant combinations (Fig. 1A,B, Table S1). These phenotypes are caused by the concurrent lack of the three TFs, as *athb2-1* loss-of-function mutants did not show differences in root length, RAM size and organization compared with the wild type (Fig. S1, Table S1). In addition, lack of ATHB2 did not aggravate the phenotype of *hat3* mutants (Fig. S1, Table S1). Only *athb4-1 athb2-3* displayed defects in RAM organization similar to those observed in *hat3 athb4*, although with reduced severity (Table S1). Interestingly, the introgression of *athb2-2* gain-of-function mutation or *ATHB2::ATHB2:GUS* construct in *hat3-3 athb4-1* were able to fully rescue the root length and RAM size without complementing QC/CC patterning defects (Fig. S1, Table S1).

We next wondered whether the irregular organization of stem cells in *hd-zip II* mutants was caused by altered development of the embryo root pole. To this end, we analyzed early embryos from heterozygous *hat3-3*$^{(-/+)}$ *athb4-1*$^{(-/-)}$ and *hat3-3*$^{(-/+)}$ *athb4-1*$^{(-/-)}$ *athb2-3*$^{(-/-)}$ genotypes. We restricted the analysis to embryos up to the transition stage as the asymmetric division of the hypophysis that specifies the root pole occurs at this stage in the wild type (Friml et al., 2003). In the progeny of *hat3-3*$^{(-/+)}$ *athb4-1*$^{(-/-)}$, about 25% of the embryos already displayed aberrant divisions of the hypophysis, as expected by the segregation of a single recessive mutation (Fig. S2). In the segregating progeny of *hat3-3*$^{(-/+)}$ *athb4-1*$^{(-/-)}$ *athb2-3*$^{(-/-)}$, the phenotype was more severe as approximately one-quarter of the embryos displayed aberrant divisions of the hypophysis and of suspensor cells (Fig. 1E,F). Together, these data indicate that HAT3, ATHB4 and ATHB2 regulate root patterning and development from embryogenesis onwards.

HAT3, ATHB4 and ATHB2 are expressed in the RAM

To investigate HD-Zip II TF expression patterns in the RAM, we generated transgenic lines expressing fluorescent protein fusions for each TF. Because *HAT3::HAT3:GFP* was unable to fully rescue *hat3 athb4* distal RAM phenotypes (Fig. S1, Table S1, Fig. 3E), we

Development (2024) 151, dev202586. doi:10.1242/dev.202586

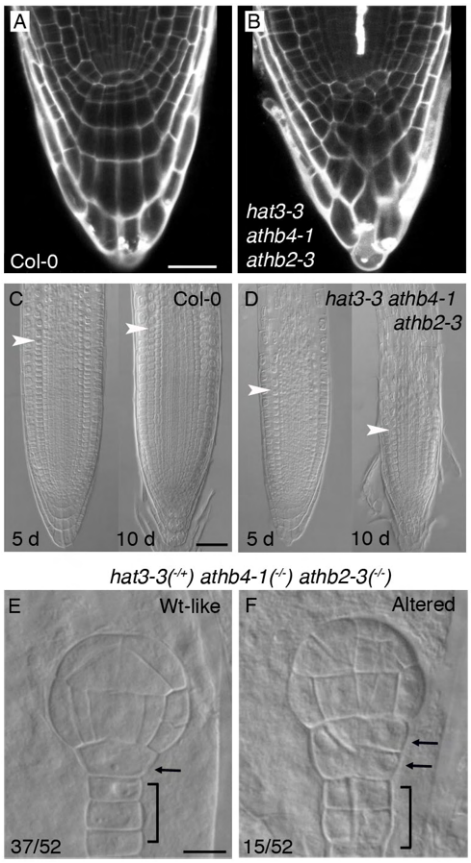

Fig. 1. HD-Zip II TFs control root patterning. (A,B) Altered SCN patterning in *hat3-3 athb4-1 athb2-3* (B) compared with Col-0 (A), as visualized using propidium iodide (PI) staining. (C,D) Reduced root apical meristem length in *hat3-3 athb4-1 athb2-3* (D) compared with Col-0 (C) in 5- and 10-day-old seedlings. Arrowheads indicate meristem boundaries. (E,F) Segregating *hat3-3*$^{(-/+)}$ *athb4-1*$^{(-/-)}$ *athb2-3*$^{(-/-)}$ embryos showing altered root pole and enhanced divisions in ~25% of the population (F) compared with wild-type-like siblings (E). Arrows and brackets mark hypophysis and suspensor, respectively. Scale bars: 5 µm in A,B; 50 µm in C,D; 20 µm in E,F.

generated constructs containing the entire genomic *HAT3*, *ATHB4* and *ATHB2* sequences, including the 3′ untranslated region (UTR), under the control of their specific promoters (respectively, 4.7 kb, 4.6 kb and 5.4 kb upstream of ATG), in which the fluorescent protein marker was inserted with a poly-Alanine linker between the stop codon and the 3′ UTR (*HAT3::HAT3:YFP; ATHB4::ATHB4:GFP*; *ATHB2::ATHB2:GFP*; Fig. S3A-C). Confocal analyses of HAT3:YFP, ATHB4:GFP and ATHB2:GFP expression patterns in the RAM showed that the three HD-Zip II proteins were predominantly expressed in the vascular tissue. ATHB2:GFP and HAT3:YFP were also detected in the pericycle (Fig. 2A-G, Table S2). In distal tissues, the expression patterns of HD-Zip II TFs were largely overlapping, although with major differences in protein levels. Of the triplet, ATHB2:GFP displayed the highest expression, whereas HAT3:YFP and ATHB4:GFP levels were extremely low, often at the limit of confocal microscopy detection. Of relevance, the differences in the expression of HD-Zip II marker lines are coherent with tissue-specific transcript levels for each gene (Fig. S3D). ATHB2:GFP expression was detected in CSCs, the first two layers of the CCs and, at a minor frequency, in the QC and Epi/LRC initials (Fig. 2C,F,G, Table S2). ATHB4:GFP expression was similar to that of ATHB2:GFP, except for the absence of signals in the QC and Epi/LRC initials (Fig. 2B,E,G; Table S2). HAT3:YFP signals were observed in CSC and CC, with an expression peak in the last columella tier. HAT3:YFP was also detected in the epidermis, LRC and their initials (Fig. 2A,D,G; Table S2). It is worth mentioning that HD-Zip II TF expression in distal RAM is highly dynamic, as we rarely observed homogeneous fluorescent signals in all the nuclei within these tissues, in particular in CSCs. To better understand HD-Zip II TF dynamics in distal stem cells, we focused on ATHB2:GFP because of its relatively high expression. We observed that ATHB2:GFP is induced in CSCs before the ACD and it is switched off in the resulting apical cell thereafter, while remaining expressed in the basal daughter, which will later differentiate into a CC (Fig. S4).

Together, these data indicate that distal RAM phenotypes observed in multiple HD-Zip II mutants are likely caused by the lack of cell-autonomous functions of these factors. In fact, HAT3:GFP, which is unable to complement patterning defects in *hd-zip II* mutants, is not detectable in distal root tissues, while the complementing HAT3:YFP protein can be detected in CSCs/CCs (Fig. 3E, Fig. S3E,F). The distal patterning defects, together with ATHB2:GFP expression dynamics in these tissues, suggest that HD-Zip II TF function is related to distal stem cell divisions.

HAT3, ATHB4 and ATHB2 regulate columella stem cell maintenance

To better understand the role of HD-Zip II TFs in distal stem cells, we carried out Lugol's starch staining to analyze the extent of CC differentiation in *hd-zip II* mutants. Depending on the phase of the cell cycle, wild-type columella contains one or two layers of CSCs, the one farther from the QC is constituted by undifferentiated CSC daughter cells (CSC-like) that will shortly expand and accumulate starch as part of their differentiation into CCs (Bennett et al., 2014). Compared with the wild type, *hat3 athb4* mutants display a reduced number of roots with two layers of CSCs, an increased number of roots with one layer and the appearance of roots with no CSCs, as deduced by the appearance of starch granules in cells adjacent to the QC. This phenotype was completely rescued by introducing *HAT3::HAT3:YFP* in the double mutant background (Fig. 3E). In *hat3-3 athb4-1 athb2-3* mutants, we observed the complete absence of RAMs with two layers of CSCs and a significant increase in the frequency of those without CSCs (Fig. 3B,C,E). These phenotypes were not observed in *hat3-3 athb2-3* and *athb4-1 athb2-3* mutants, indicating that the presence of either HAT3 or ATHB4 is sufficient for CSC maintenance (Fig. S5). Consistently, the expression of ATHB4:GFP in *hat3-3 athb4-1 athb2-3* restored the CSC phenotype to wild-type levels (Fig. 3E). In contrast, the expression of ATHB2:GFP in *hat3-3 athb4-1 athb2-3* could only restore the phenotype to the levels of *hat3-3 athb4-1* (Fig. 3E). Notably, the gain-of-function *athb2-2*, which expresses increased levels of *ATHB2* (Turchi et al., 2013), displays a higher percentage of roots with two layers of CSCs compared with the wild type (Fig. 3A,D,E).

The enhanced CC differentiation observed in *hd-zip II* mutants (Fig. 3A,B,E) is suggestive of a reduction in CSC proliferation. Thus, we used the thymidine analogue F-ara-EdU (Bennett et al., 2014; Hong et al., 2015) to study cell cycle progression and proliferation in the columella. We analyzed F-ara-EdU incorporation in wild type, *hat3-3 athb4-1*, *hat3-3 athb4-1 athb2-3* and *athb2-2* mutants, and quantified the number of DNA replication and cell division events at the QC (*q*), CSC (*c1*) and the first layer of CC (*c2*) positions (Fig. 3K-N). Compared with the wild type, loss- (*hat3-3 athb4-1*, *hat3-3 athb4-1 athb2-3*) and gain-of-function (*athb2-2*) mutants showed reduced and enhanced cell cycle progression at *c1*, respectively (Fig. 3K-N, Table 1). In addition, reductions in cell

Development (2024) 151, dev202586. doi:10.1242/dev.202586

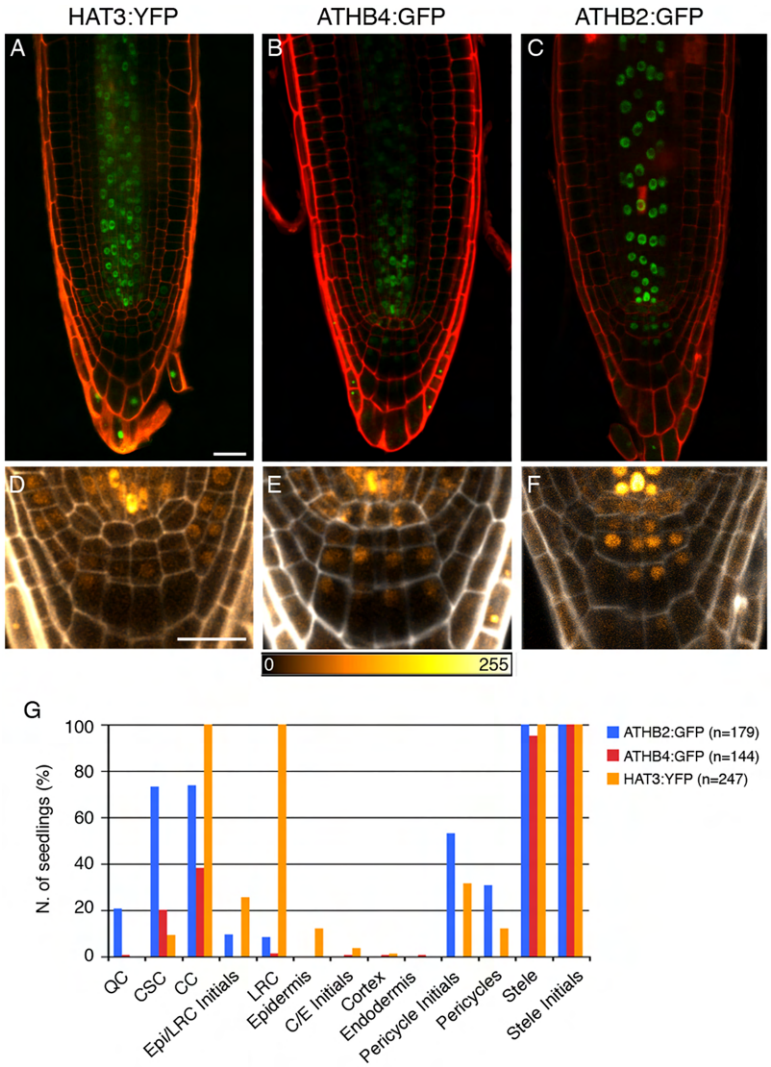

Fig. 2. HD-Zip II TFs are expressed in the root meristem. (A-C) Expression of HAT3:YFP (A), ATHB4:GFP (B) and ATHB2:GFP (C) proteins (green) in wild-type roots. (D-F) Details of HAT3:GFP (D), ATHB4:GFP (E) and ATHB2:GFP (F) expression in distal tissues of the roots in A-C, using the color scale indicated. PI counterstaining: red (A-C) and gray (D-F). Scale bars: 20 µm. (G) HD-Zip II protein distribution within meristematic tissues expressed as a percentage of roots displaying fluorescence in indicated cell types (see Table S2). C/E, cortex/endodermis.

division at *c1* were observed in *hat3-3 athb4-1* and, to a greater extent, in *hat3-3 athb4-1 athb2-3* compared with the wild type. Noteworthy, *athb2-2* gain-of-function mutants displayed enhanced cell cycle progression and cell division also at *q* position, indicating that moderate increases in *ATHB2* expression promote CSC and QC proliferation (Table 1). Together, Lugol's and F-ara-EdU analyses show that HD-Zip II proteins play a role in CSC maintenance. Consistently, the expression of the CSC-specific marker J2341 was severely compromised in *hat3-3 athb4-1 athb2-3*, indicating the loss of stem cell identity in absence of HD-Zip II TFs (Fig. 3F-J).

Overall, these data demonstrate that HD-Zip II TFs maintain the identity and function of CSCs by sustaining their proliferative status. The genetic analyses demonstrate that the presence of either HAT3 or ATHB4, but not of ATHB2, is necessary for CSC maintenance. However, ATHB2 function positively correlates with stem cell proliferation, as higher *ATHB2* levels in the gain-of-function mutant increase QC and CSC proliferation.

HAT3, ATHB4 and ATHB2 interfere with auxin response to regulate CSC activity

Auxin regulates the formation of the columella during the embryogenesis, as well as its maintenance and differentiation in post-embryonic roots (Ding and Friml, 2010; Dubreuil et al., 2018; Friml et al., 2003; Weijers et al., 2006). We thus wondered whether distal RAM defects observed in *hd-zip II* mutants were due to altered auxin distribution or response. We analyzed the expression pattern of the *DR5rev::GFP* auxin response marker in relation to aberrant hypophysis division in *hat3-3*$^{(-/+)}$ *athb4-1*$^{(-/-)}$ segregating embryos. In globular embryos displaying altered root pole, *DR5rev::GFP* expression was markedly reduced in hypophysis and increased in suspensor cells, as opposed to wild-type-like embryos, which displayed only DR5 signals in the hypophysis (Fig. S6). These results suggest that altered root pole development in *hat3 athb4* is caused by a defective establishment of auxin maxima. However, in *hat3 athb4* mature embryos (Turchi et al., 2013) and in post-embryonic roots, *DR5rev::GFP* expression does not differ substantially from the wild type (Fig. S6).

Next, we analyzed *DR5rev::GFP* post-embryonic expression pattern in *hat3 athb4 athb2* mutant roots. Despite the severe CSC phenotypes, *hat3-3 athb4-1 athb2-3* did not display at a first glance major differences in DR5 expression compared with the wild type (Fig. 4A,B). However, upon quantitative analyses of DR5 expression, we could highlight differences between the wild type and the triple mutant. In particular, in *hat3 athb4 athb2*, DR5

Development (2024) 151, dev202586. doi:10.1242/dev.202586

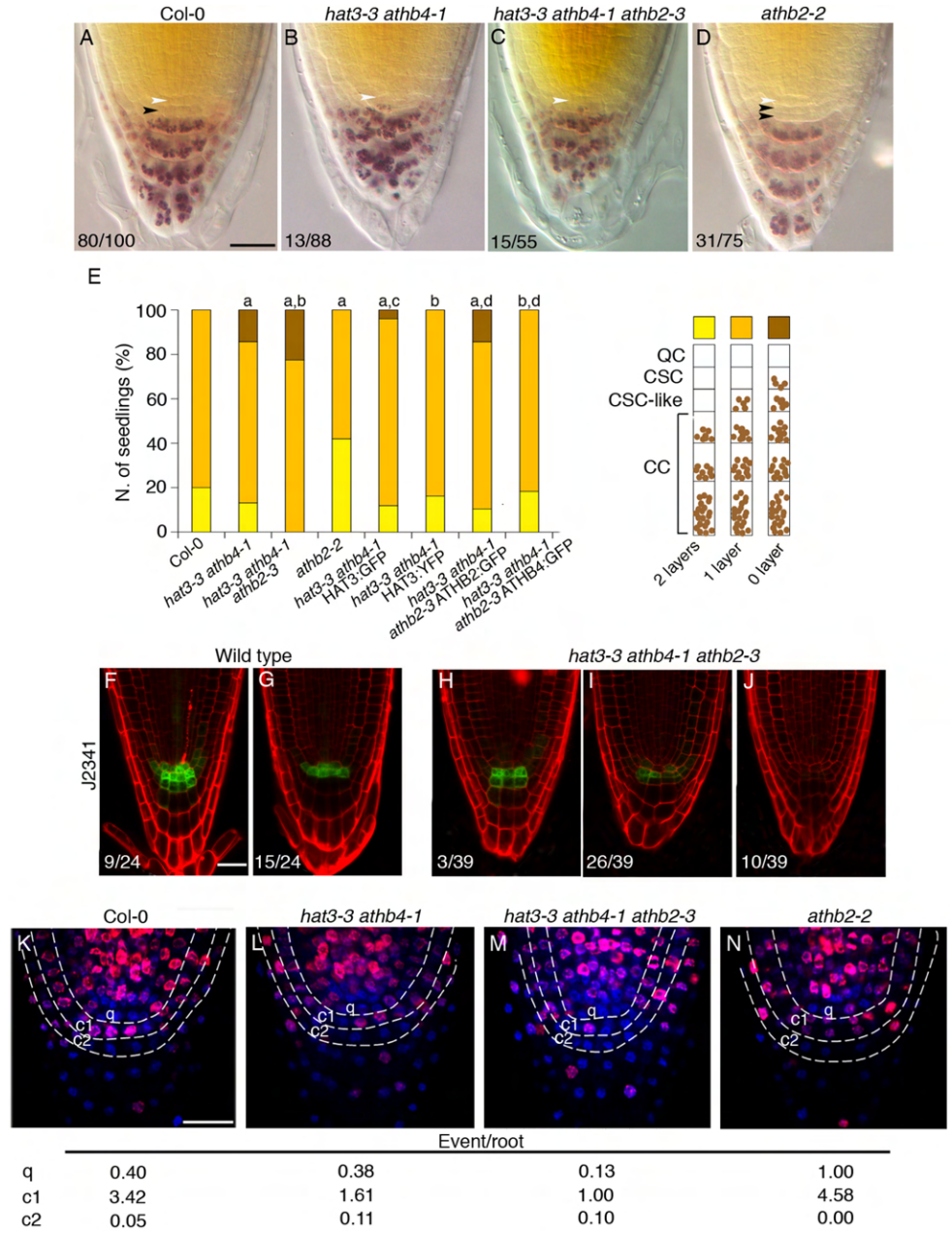

Fig. 3. HD-Zip II TFs regulate columella stem cell fate and identity. (A-D) Lugol's staining in Col-0 (A), *hat3-3 athb4-1* (B), *hat3-3 athb4-1 athb2-3* (C) and *athb2-2* (D). Arrowheads: white, quiescent center (QC); black, columella stem cells (CSCs). (E) Number of CSC layers in the indicated genotypes, according to the scheme on the right. [a]*P*<0.01 versus Col-0; [b]*P*<0.01 versus *hat3-3 athb4-1*; [c]*P*<0.01 versus *hat3-3 athb4-1 athb2-3*. (F-J) J2341 expression in wild-type (F,G) and *hat3-3 athb4-1 athb2-3* (H-J) roots. Ratios indicate frequencies of depicted expression patterns. (K-N) F-ara-EdU incorporation (magenta) in Col-0 (K), *hat3-3 athb4-1* (L), *hat3-3 athb4-1 athb2-3* (M) and *athb2-2* (N) roots counterstained with DAPI (blue). The event/root index highlights differences in S-phase progression (see Table 1). Scale bars: 5 µm in A-D; 20 µm in F-N.

expression increased in the CSCs with a slight, albeit non-significant, decrease in the QC compared with the wild type (Fig. 4A-C). Because the expression pattern of the auxin biosynthesis reporter *TAA1::GFP:TAA1* was only slightly affected in *hat3 athb4 athb2* compared with the wild type (Fig. S7), we wondered whether the shift in DR5 expression could be attributable to altered auxin transport. To this end, we analyzed the expression of *PIN3*, *PIN4* and *PIN7* auxin efflux carriers in *hat3-3 athb4-1 athb2-3*. We found that the expression of PIN3:GFP and PIN4:GFP, but not that of PIN7:GFP, was enhanced in the triple mutant compared with the wild type (Fig. 4D-J). The increase in PIN3 and PIN4 levels was particularly evident in distal tissues where they play a key role in the maintenance of auxin maximum and columella differentiation (Blilou et al., 2005; Ding and Friml, 2010). To test whether altered expression of PINs contributes to *hd-zip II* distal stem cells defects, we analyzed CSC phenotypes in multiple *hd-zip II pin* mutant combinations. In contrast to *pin3-4*, *pin4-3* and *pin7-2* single mutants, showing higher frequencies of RAMs with two CSC layers

Development (2024) 151, dev202586. doi:10.1242/dev.202586

Table 1. Quantification of F-ara-EdU incorporation in the genotypes used in this study

	Position	Replication	Division	Event/root
Col-0	*q*	14	0	0.40
(*n*=35)	*c1*	56	64	3.42
	c2	2	0	0.05
hat3-3	*q*	14	0	0.38
athb4-1	*c1*	41	17	1.61[a]
(*n*=36)	*c2*	4	0	0.11
hat3-3	*q*	4	0	0.13[b]
athb4-1	*c1*	22	8	1.00[a,c]
athb2-3	*c2*	3	0	0.10
(*n*=30)				
athb2-2	*q*	18	8	1.00[d]
(*n*=26)	*c1*	59	60	4.58[a]
	c2	0	0	0.00
wox5-1	*q*	35	14	1.53[a]
(*n*=32)	*c1*	28	4	1.00[a]
	c2	3	0	0.09
hat3-3	*q*	21	12	1.26[a]
athb4-1	*c1*	12	0	0.46[a,d,e]
athb2-3	*c2*	2	0	0.07
wox5-1				
(*n*=26)				
fez-2	*q*	15	2	0.60
(*n*=28)	*c1*	30	9	1.39[a]
	c2	6	0	0.21
hat3-3	*q*	9	0	0.29
athb4-1	*c1*	30	2	1.03[a]
athb2-3	*c2*	4	0	0.12
fez-2				
(*n*=31)				
smb-3	*q*	15	0	0.55
(*n*=27)	*c1*	58	22	2.96
	c2	35	9	1.62[a]
hat3-3	*q*	6	0	0.19[b]
athb4-1	*c1*	27	6	1.06[a]
athb2-3	*c2*	5	1	0.19[f]
smb-3				
(*n*=31)				

The number of DNA replication and cell division events was quantified by counting F-ara-EdU-positive nuclei at indicated positions. The final column shows sum of replications and divisions, divided by the number of roots. [a]*P*<0.01 versus Col-0; [b]*P*<0.05 versus Col-0; [c]*P*<0.01 versus *hat3-3 athb4-1*; [d]*P*<0.05 versus *hat3-3 athb4-1 athb2-3*; [e]*P*<0.05 versus *wox5-1*; [f]*P*<0.01 versus *smb-3*.

compared with the wild type (Blilou et al., 2005; Ding and Friml, 2010; Friml et al., 2002b), quadruple mutant combinations *hat3-3 athb4-1 athb2-3 pin3-4*, *hat3-3 athb4-1 athb2-3 pin4-3* and *hat3-3 athb4-1 athb2-3 pin7-2* displayed enhanced CSC differentiation like the triple *hd-zip II* (Fig. 4K). Thus, increased expression of PINs in CCs is unlikely to be the cause of enhanced CSC differentiation in *hat3 athb4 athb2*.

We next tested whether alterations in auxin signaling mediated by TRANSPORT INHIBITOR RESISTANT 1/AUXIN BINDING F-BOX (TIR1/ABF) receptors could explain *hd-zip II* mutant phenotypes. We analyzed the effect of auxinole, a potent auxin antagonist of TIR1/AFBs receptors (Hayashi et al., 2008, 2012), on wild-type and *hat3 athb4 athb2* roots. In the wild type, auxinole treatments increased the frequency of RAMs with two layers of CSCs compared with untreated controls, in agreement with an expected inhibition of auxin-mediated CC differentiation. In *hat3-3 athb4-1 athb2-3*, auxinole restored the occurrence of RAMs with two layers of CSCs normally absent in this background (Fig. 4L), suggesting that HD-Zip II TFs might regulate CSC activity by counteracting auxin signaling. Thus, we expressed ATHB4 under the control of a β-estradiol inducible system (*XVE>ATHB4*) to test whether high levels of a HD-Zip II TF counteract the auxin-mediated CSC differentiation. Consistent with the phenotype of the gain-of-function *athb2-2*, high levels of ATHB4 enhanced CSC proliferation (Fig. 4M, Fig. S8) and cell cycle progression at *c1* in β-estradiol-treated versus untreated plants (Fig. S8, Table S3). Remarkably, the application of NAA did not enhance CSC differentiation upon induction of ATHB4, as observed in uninduced controls (Fig. 4M). Together, these data indicate that HD-Zip II TFs regulate CSC fate by affecting the cellular readout of auxin signaling.

HD-Zip II TFs interfere with the ARF10/ARF16 pathway, but not with WOX5, to regulate CSC activity downstream of auxin

Auxin-mediated CSC differentiation has been linked to the action of WOX5 (Bennett et al., 2014; Ding and Friml, 2010; Savina et al., 2020). To understand whether WOX5 contributes to HD-Zip II functions in distal stem cells, we analyzed *WOX5::GFP* expression in *hat3 athb4 athb2* and found that it was substantially unchanged compared with the wild type (Fig. 5A,B). We thus wondered whether HD-Zip II TFs, which act as transcriptional repressors (Steindler et al., 1999), could be involved in the auxin-mediated downregulation of WOX5 expression. Interestingly, we observed that ATHB2:GFP is significantly upregulated by NAA treatments in the RAM (Fig. 5J,K). In distal tissues, NAA increased the frequency of QC and CSC cells expressing ATHB2:GFP at a given time (Fig. 5K, Fig. S9), suggesting that auxin stabilizes ATHB2 expression dynamics in distal tissues. However, the *WOX5::GFP* transcriptional response to NAA did not differ between the wild type and the triple mutant (Fig. 5C,D), indicating that the auxin-mediated *WOX5* downregulation is independent of HD-Zip II TFs. Consistently, Lugol's and F-ara-Edu analyses demonstrated the additivity of the *hat3 athb4 athb2 wox5* mutant phenotypes, indicating that HD-Zip II TFs and WOX5 regulate CSC activity through parallel pathways (Fig. 5E-I).

To further investigate the link between auxin and HD-Zip II TFs, we focused on ARF10 and ARF16, the double loss-of-function mutant of which displays uncontrolled cell division and impaired cell differentiation in the distal RAM (Wang et al., 2005). To test the genetic relationship between HD-Zips II and ARF TFs, we generated and analyzed the *hat3-3 athb4-1 athb2-3 arf10-2 arf16-2* quintuple mutant. The phenotype of *hat3-3 athb4-1 athb2-3 arf10-2 arf16-2* showed mitigation of the uncontrolled cell proliferation with fewer layers of undifferentiated cells with CSC morphology compared with the parental *arf10 arf16* (Fig. 5M-P), suggesting that HD-Zip II TFs contribute to the increased CSC proliferation of *arf10 arf16*. Consistently, we found that ATHB2:GFP is expressed in an enlarged domain of *arf10 arf16* distal RAM compared with the wild type (Fig. 5Q,R). In addition, we found that the *pARF10::n3GFP* expression domain, which is restricted to the Epi/LRC initials in distal tissues of the wild type, expands toward CSCs and CCs in *hat3 athb4 athb2* (Fig. 5S,T). Conversely, the expression of *pARF16::*

Development (2024) 151, dev202586. doi:10.1242/dev.202586

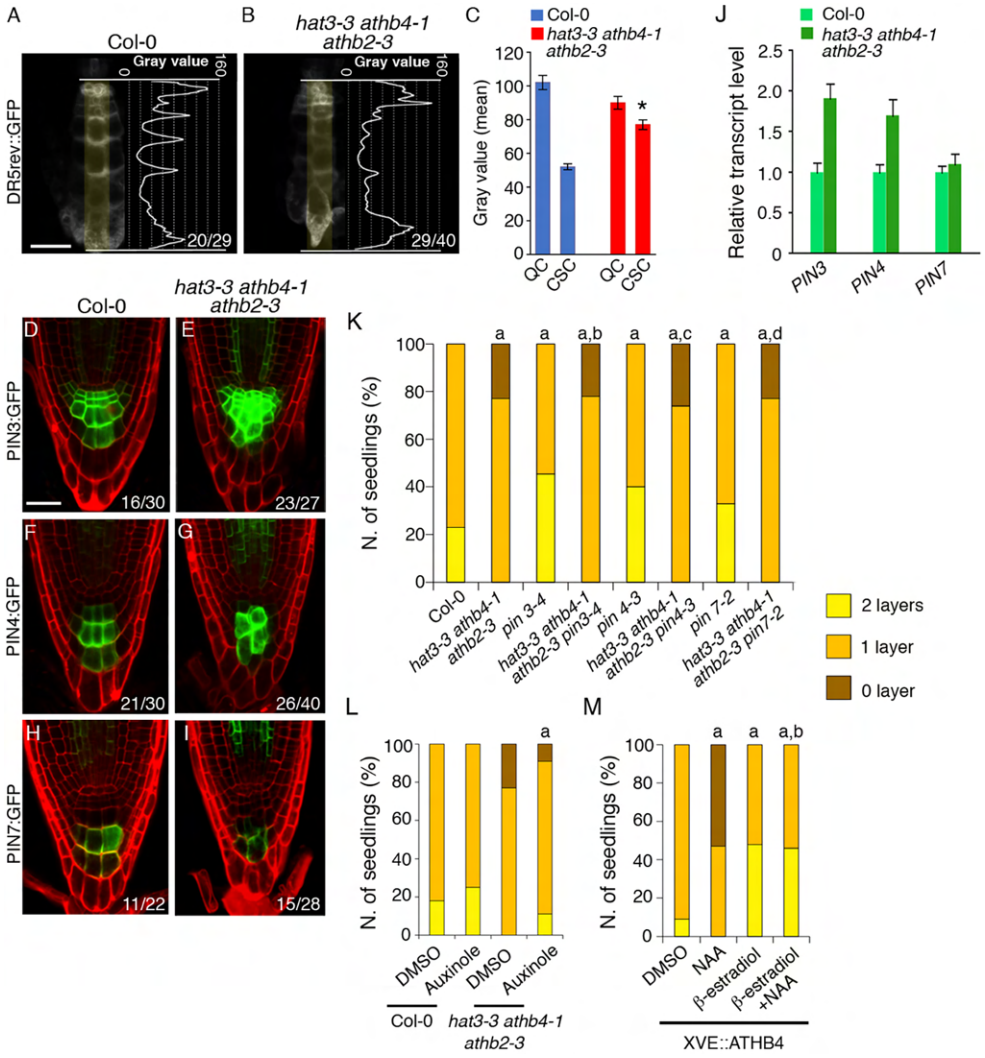

Fig. 4. HD-Zip II TFs affect auxin transport and signaling in the RAM. (A-C) *DR5rev::GFP* expression in Col-0 (A) and *hat3-3 athb4-1 athb2-3* (B) displayed with signal intensity profiles measured along the highlighted regions. (C) Quantification of *DR5rev::GFP* intensity in the Col-0 and *hat3-3 athb4-1 athb2-3* quiescent center (QC) and columella stem cells (CSCs). **P*<0.01 versus Col-0 CSC. Data are mean fluorescence intensity (gray value)±s.e.m. (D-I) PIN3:GFP (D,E), PIN4:GFP (F,G) and PIN7:GFP (H,I) expression in Col-0 (D,F,H) and *hat3-3 athb4-1 athb2-3* (E,G,I). Scale bars: 20 µm. Ratios indicate the frequencies of depicted expression patterns. (J) Relative expression levels of *PIN3*, *PIN4* and *PIN7* in Col-0 and *hat3-3 athb4-1 athb2-3* roots determined by qRT-PCR. Data are mean relative transcript levels±s.d. (*n*=3). (K) Number of CSC layers in multiple *hd-zip II pin* mutant combinations. [a]*P*<0.01 versus Col-0; [b]*P*<0.01 versus *pin3-4*; [c]*P*<0.01 versus *pin4-3*; [d]*P*<0.01 versus *pin7-2*. (L) Number of CSC layers in Col-0 or *hat3-3 athb4-1 athb2-3* treated with DMSO or 5 µM auxinole. [a]*P*<0.01 versus *hat3-3 athb4-1 athb2-3* DMSO. (M) Induction of ATHB4 inhibits auxin-mediated CSC differentiation. Number of CSC layers in *XVE>ATHB4* treated as indicated. [a]*P*<0.01 versus DMSO; [b]*P*<0.01 versus NAA.

n3GFP is specifically downregulated in the CSCs/CCs of the *hat3 athb4 athb2* mutant compared with the wild type (Fig. 5U,V). Together, these data suggest an interdependency of HD-Zip II TFs and ARFs in controlling the balance between proliferation and differentiation in distal stem cells.

HD-Zip II TFs act downstream of the FEZ/SMB loop to control CSC proliferation

As the genetic interaction with ARFs cannot fully explain the phenotypes observed in *hat3 athb4 athb2*, we next tried to determine whether HD-Zip II TFs connect with FEZ and SMB, key players of stem cell fate and patterning in the root cap (Willemsen et al., 2008). To gain insights on the interactions among HD-Zip II proteins and the FEZ/SMB pathway, we generated the quadruple mutants *hat3-3 athb4-1 athb2-3 fez-2* and *hat3-3 athb4-1 athb2-3 smb-3*. Lugol's analysis showed that the *hat3-3 athb4-1 athb2-3 fez-2* quadruple mutant displays the same phenotype as *fez-2* (Fig. 6A). F-ara-EdU experiments showed that cell cycle progression at *c1* is slightly slower, although not in a significant manner, in *hat3-3 athb4-1 athb2-3* than in *fez-2* with respect to wild type. In addition, the proliferative activity of *hat3-3 athb4-1 athb2-3 fez-2* resembles that of *hat3-3 athb4-1 athb2-3* (Fig. 6 B-E, Table 1), suggesting that HD-Zip II TFs and FEZ act in the same pathway. We further analyzed the expression of FEZ:GFP in *hat3-3 athb4-1 athb2-3* and found no significant difference between the triple mutant and the wild type (Fig. 6H,I). On the other hand, ATHB2:GFP was not expressed in root cap tissues of the *fez-2* mutant (Fig. 6J,K). Importantly, ATHB2:GFP expression could not be

Development (2024) 151, dev202586. doi:10.1242/dev.202586

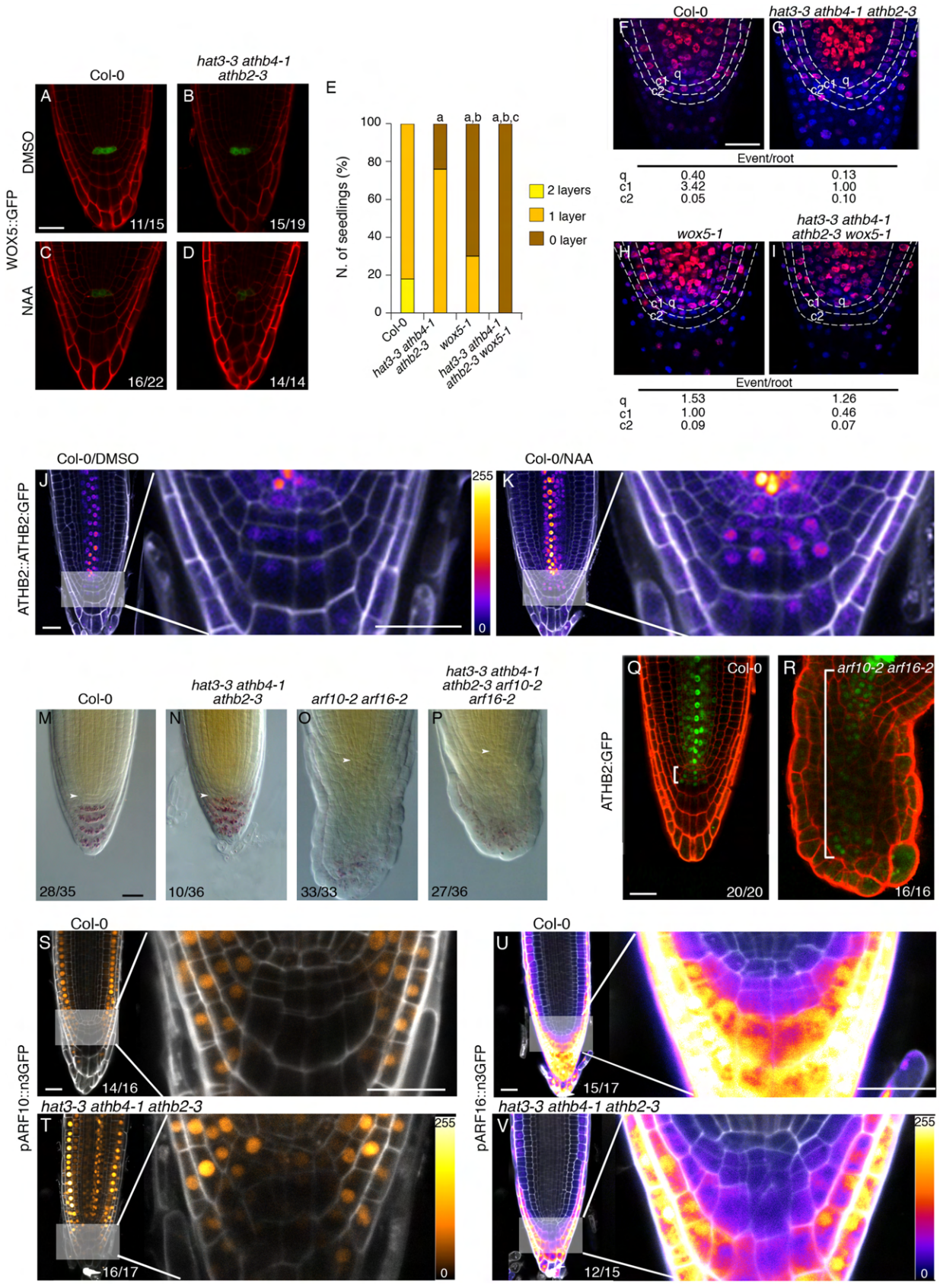

Fig. 5. See next page for legend.

Development (2024) 151, dev202586. doi:10.1242/dev.202586

Fig. 5. Genetic interactions between HD-Zip II TFs and auxin-related CSC regulators WOX5 and ARF10/ARF16. (A-D) *WOX5::GFP* expression in Col-0 (A,C) and *hat3-3 athb4-1 athb2-3* (B,D) roots, untreated (A,B) or treated with NAA (C,D). (E) Number of CSC layers in the indicated genotypes. [a]*P*<0.01 versus Col-0; [b]*P*<0.01 versus *hat3-3 athb4-1 athb2-3;* [c]*P*<0.01 versus *wox5-1*. (F-I) F-ara-EdU incorporation in Col-0 (F), *hat3-3 athb4-1 athb2-3* (G), *wox5-1* (H) and *hat3-3 athb4-1 athb2-3 wox5-1* (I) roots counterstained with DAPI. The event/root index highlights differences in S-phase progression (see Table 1). (J,K) ATHB2:GFP expression in roots treated for 24 h with DMSO (J) or NAA (K), with details of distal tissues. GFP is displayed using the color scale in the inset. (M-P) Lugol-stained roots of Col-0 (M), *hat3-3 athb4-1 athb2-3* (N), *arf10-2 arf16-2* (O) and *hat3-3 athb4-1 athb2-3 arf10-2 arf16-2* (P). Arrowheads indicate the quiescent center (QC). (Q,R) Extension of ATHB2:GFP expression domains (square bracket) in Col-0 (Q) and *arf10-2 arf16-2* (R) distal tissues. (S-V) Expression of *pARF10::n3GFP* (S,T) and *pARF16::n3GFP* (U,V) in Col-0 (S,U) and *hat3-3 athb4-1 athb2-3* (T,V) roots, with details of distal tissues. GFP is displayed using the color scale in insets. Ratios indicate frequencies of depicted expression patterns. Scale bars: 20 µm in A-D,F-K,Q-V; 5 µm in M-P.

restored in distal tissues even in the presence of NAA (Fig. 6M,N), indicating that FEZ is required for the auxin-mediated induction of ATHB2. Based on these results, we hypothesized that the strong reduction in cell cycle progression at *c1* in *fez* mutant might be caused by the loss of HD-Zip II TF expression. To verify this hypothesis, we introduced in the *fez-2* background the *35S::HAT3:GR* construct expressing a dexamethasone (DEX)-inducible version of HAT3. We chose HAT3 because, similarly to ATHB2, its expression is not detectable in *fez-2* CSCs and CCs (Fig. S10). Upon DEX induction, HAT3:GR was able to fully complement *hat3-3 athb4-1 athb2-3* CSC phenotypes, confirming the functionality of the chimeric protein (Fig. 6O-Q). Remarkably, HAT3:GR was able to largely recover the CSC phenotype of *fez-2* upon DEX induction (Fig. 6O-Q), indicating that FEZ activity on CSC proliferation largely depends on HD-Zip II TFs.

We next analyzed the interactions between HD-Zip II TFs and SMB. Lugol's analysis showed that CSC differentiation is delayed in *smb-3* mutant (Fig. 6A). F-ara-Edu analysis showed that the number of mitotic events at *c2* is significantly increased in *smb-3* compared with the wild type, implying that, in absence of SMB, CSC daughters maintain stem cell fate and undergo an extra round of division (Fig. 6B,F, Table 1). Coherently, we found that, in *smb-3* mutants, ATHB2:GFP was predominantly expressed in *c2-c3* layers, following the proliferative pattern of distal cells (Fig. 6J,L), which mirrors the expanded FEZ domain observed in *smb-3* (Willemsen et al., 2008). Interestingly, the enhanced proliferation of *smb-3*, which is caused by high levels of FEZ (Willemsen et al., 2008), was recovered by the lack of HD-Zip II TFs, as quadruple *hat3-3 athb4-1 athb2-3 smb-3* mutants display essentially the same phenotype of *hat3-3 athb4-1 athb2-3* (Fig. 6B,C,F,G; Table 2). This implies that FEZ-mediated proliferation requires HAT3, ATHB4 and ATHB2 functions. Together, the combination of genetic and expression data strongly suggests that the three HD-Zip II TFs act as effectors of the FEZ/SMB loop in controlling CSC proliferation.

DISCUSSION

The maintenance of the SCN in the *Arabidopsis* root tip is precisely regulated by multiple independent pathways that impinge quantitatively on the processes governing the switch between proliferation and differentiation (Bennett et al., 2014). Here, we provide evidence that HAT3, ATHB4 and ATHB2, originally identified as regulators of plant responses to canopy shade (reviewed by Ruberti et al., 2012; Sessa et al., 2018), are involved in the patterning of distal root tissues by controlling root pole formative divisions during embryogenesis and the CSC proliferation/differentiation balance in post-embryonic development. Regarding the latter aspect, our work shows that the three HD-Zip II TFs play a role in promoting distal stem cell proliferation, as confirmed by the enhanced CSC differentiation in double and triple mutants. Although HAT3, ATHB4 and ATHB2 seem not completely redundant in the process, increased expression of either one consistently promotes CSC proliferation (Figs 3, 4 and 6, Table 1), indicating that the three TFs are interchangeable to some extent and likely share the same targets in the regulation of stem cell maintenance. HD-Zip II TFs do not function as another independent pathway; rather, they take part in the regulatory circuitry underlying distal stem cell maintenance by connecting the auxin and the FEZ/SMB pathways.

The FEZ/SMB pathway represents a core mechanism setting the pace of the CSC division/differentiation decision-making process and relies on a precise feedback loop between the two NAC TFs across adjoining root cap cell layers, with SMB promoting differentiation by repressing FEZ-mediated proliferative activity (Bennett et al., 2014; Willemsen et al., 2008). Interestingly, FEZ activity promotes CSC proliferation, although the protein itself is not strictly required for cell division (Bennett et al., 2014). In this framework, our results suggest that HD-Zip II TFs act as an effector of FEZ in the regulation of CSC proliferation. Several lines of evidence support this hypothesis: FEZ-mediated proliferation in *smb* requires HD-Zip II functions; FEZ is required for the expression of ATHB2 and HAT3; and inducing HAT3:GR expression restores CSC proliferation in *fez* mutants. Noteworthy, the cycling expression pattern of ATHB2 across CSCs and daughter cells, as well as its expanded expression domain in *smb*, mirrors those reported for FEZ (Willemsen et al., 2008), further suggesting that FEZ could be directly involved in the regulation of *ATHB2* and the other HD-Zip II TFs. Of relevance, FEZ activity has been shown to be sufficient to redirect the plane of cell division in other root tissues or during wound repair processes (Marhava et al., 2019; Willemsen et al., 2008). Similarly, ectopic expression of ATHB4 and HAT3 promotes periclinal division in epidermis, cortex, endodermis and pericycle cells (Fig. S8), suggesting that the interplay of HD-Zip II TFs and FEZ could occur even outside the CSCs and, most importantly, it could regulate cell division planes in the embryo root pole.

Our results further indicate that HD-Zip II TFs regulate distal stem cell proliferation by counteracting the auxin-induced CSC differentiation. Two main lines of evidence support this view: the enhanced differentiation of CSCs in the triple *hd-zip II* mutant can be dampened by inhibiting auxin signaling; overexpressing ATHB4 blocks the effect of auxin on CSC differentiation. These data clearly indicate that HD-Zip II TFs play a role in tuning down the cellular readout of auxin signaling in the root cap. In particular, the expression patterns of *ARF10* and *ARF16* are altered in the triple *hd-zip II* mutant: the former being upregulated and the latter downregulated in the mutant columella. ARF10 and ARF16 are auxin-inducible, class C (i.e. negative) ARFs that are expressed in partially overlapping domains and redundantly function to repress cell proliferation in the distal RAM (Dai et al., 2021; Mutte et al., 2018; Rademacher et al., 2011; Wang et al., 2005). ARF10 and ARF16 were proposed to repress CSC proliferation in response to auxin via WOX5 (Ding and Friml, 2010). Our genetic and molecular data show that HD-Zip II TFs are unlikely to interfere with WOX5-mediated regulation of CSC cell fate. Instead, our data suggest that the HD-Zip II TFs, by controlling the expression domains of *ARF10* and *ARF16*, modify the local perception of auxin levels, thus modulating the balance between proliferation and differentiation. It

Development (2024) 151, dev202586. doi:10.1242/dev.202586

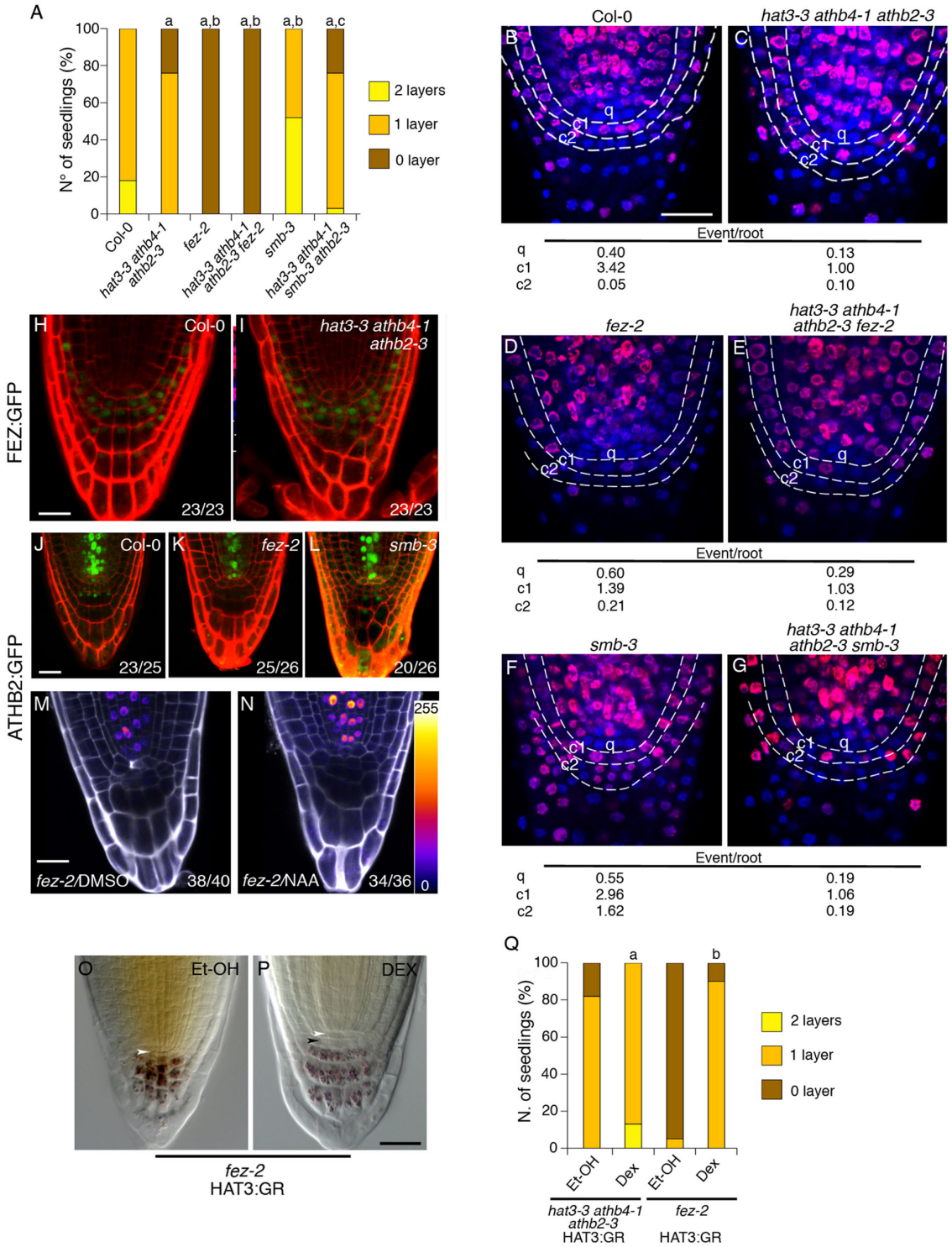

Fig. 6. HD-Zips II TFs act downstream of the FEZ/SMB pathway to regulate CSCs fate. (A) Number of columella stem cell (CSC) layers in *hd-zip II*, *fez* and *smb* mutant combinations. [a]*P*<0.01 versus Col-0; [b]*P*<0.01 versus *hat3-3 athb4-1 athb2-3*; [c]*P*<0.01 versus *smb-3*. (B-G) F-ara-EdU incorporation in Col-0 (B), *hat3-3 athb4-1 athb2-3* (C), *fez-2* (D), *hat3-3 athb4-1 athb2-3 fez-2* (E), *smb-3* (F) and *ha3-3 athb4-1 athb2-3 smb-3* (G) roots counterstained with DAPI. The event/root index highlights differences in S-phase progression (see Table 1). (H,I) FEZ:GFP expression in Col-0 (H) and *hat3-3 athb4-1 athb2-3* (I). (J-L) ATHB2:GFP expression in Col-0 (J), *fez-2* (K) and *smb-3* (L). (M,N) ATHB2:GFP expression in *fez-2* roots treated with DMSO (M) or NAA (N) for 24 h according to the color scale in the inset. Ratios indicate frequencies of depicted expression patterns. (O,P) *fez-2* HAT3:GR roots treated for 24 h with ethanol (O) or DEX (P). Arrowheads: white, quiescent center (QC); black, CSCs. (Q) Number of CSC layers in *hat3-3 athb4-1 athb2-3* HAT3:GR and *fez-2* HAT3:GR treated with ethanol or dexamethasone for 24 h. [a]*P*<0.01 versus *hat3-3 athb4-1 athb2-3* HAT3:GR/ethanol; [b]*P*<0.01 versus *fez-2* HAT3:GR/ethanol. Scale bars: 20 µm in B-N; 5 µm in O,P.

Development (2024) 151, dev202586. doi:10.1242/dev.202586

remains to be established how the opposite regulation of *ARF10* and *ARF16* by HD-Zip II TFs is achieved. A simple possibility is that HD-Zip II TFs target only ARF10, which in turn controls ARF16 expression, in line with the current view of auxin responses being regulated by networks of transcriptional repressors (Truskina et al., 2021). It must be pointed out that the activity of ARF10 and ARF16 in the CSC has been demonstrated to be regulated by IAA33 (Lv et al., 2020). IAA33, like other non-canonical AUX/IAA proteins, is stabilized by auxin and regulates the transcriptional activity of ARFs in competition with canonical, auxin-degradable AUX/IAAs (Cao et al., 2019; Lv et al., 2020). Thus, additional AUX/IAA-ARF pairs downstream of TIR1/ABFs (Lv et al., 2020; Wang et al., 2023) may be involved in the HD-Zip II-mediated regulation of auxin perception, as further suggested by the partial rescue of the *hd-zip II* mutant phenotype by auxinole. Interestingly, IAA33 was identified as a putative interactor of ATHB2 in a large-scale yeast two-hybrid screen (Wanamaker et al., 2017), suggesting more complex regulatory mechanisms linking HD-Zip II TF activity to ARF-mediated auxin responses. It must be also considered that HD-Zip II TFs may interfere with auxin signaling indirectly, by altering local hormone fluxes via the transcriptional control of PIN genes (this work; Yuan et al., 2021).

Interestingly, the expression of ATHB2 is regulated by auxin, similar to other members of the γ subfamily of HD-Zip II TFs (He et al., 2020; Sawa et al., 2002). Auxin induces ATHB2 and stabilizes its expression dynamics in distal tissues. The auxin-mediated regulation of ATHB2 expression does not occur in *fez* mutants (Fig. 6), suggesting that ATHB2 counteracts IAA-induced differentiation by promoting stem cell proliferation downstream of FEZ. Indeed, ATHB2 is also induced by auxin in the QC, where it stimulates divisions, as inferred by the gain-of-function mutant. The QC is known to divide to replenish differentiating CSCs, acting as a reservoir of stem cells in response to extreme stress or damage (Cruz-Ramírez et al., 2013; Heyman et al., 2013). Thus, ATHB2 upregulation may represent a feedback response to prevent exaggerated CSC differentiation in the presence of excess auxin. Taken together, our data show that HD-Zip II TFs regulate distal stem cell fate by integrating opposing inputs to fine-tune the balance between proliferation and differentiation (Fig. 7). This integration may be of primary importance to synchronize root cap growth with the environment. Auxin regulates root growth in response to different environmental conditions, including light, temperature, drought and nutrient deprivation (Ai et al., 2023; Hong et al., 2017; Liu and von Wirén, 2022; Sassi et al., 2012). In this framework, HD-Zip II TFs may act as a hub that integrates developmental cues (i.e. FEZ/SMB loop) with auxin-transmitted environmental cues to regulate distal stem cell behavior and, as a result, the dynamics of root cap growth.

It has previously been shown that HAT3, ATHB4 and ATHB2 redundantly regulate SAM activity and maintenance (Turchi et al., 2013), which, together with the findings reported here, may lead to the idea that the function of HD-Zip II TFs is to promote proliferation. However, in leaf primordia, different members of the HD-Zip II family inhibit the proliferation of mesophyll cells (Carabelli et al., 2018; Challa et al., 2019; Ciarbelli et al., 2008). Upon prolonged exposure to shade, ATHB2 and ATHB4 have been shown to slow down cell divisions, eventually resulting in mesophyll cell differentiation (Carabelli et al., 2018). Thus, the role of HD-Zip II TFs in cell fate determination seems to be context dependent: even in the proximal RAM, the induction of *XVE>HAT3* or *XVE>ATHB4* also promotes the ectopic differentiation of epidermal cells into CCs, as indicated by the accumulation of

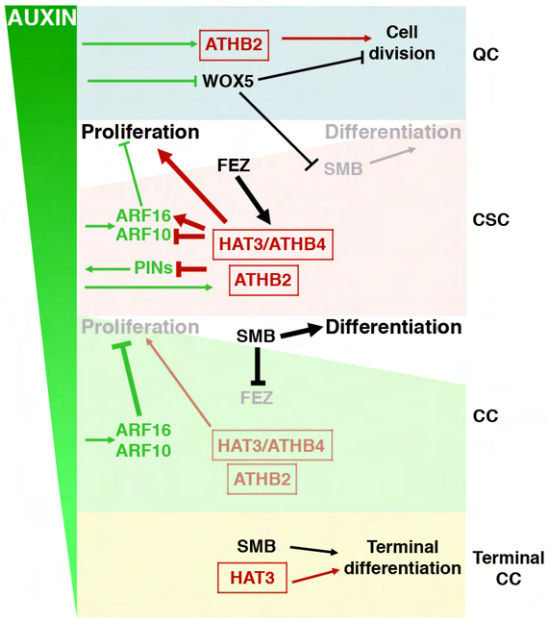

Fig. 7. A model for HD-Zip II TF function in CSC fate determination. In columella stem cells (CSCs), HD-Zip II TFs promote proliferation downstream of FEZ by interfering with auxin-mediated differentiation. On one hand, HD-Zip II TFs affect the expression of PINs to modulate auxin gradients; on the other hand, HD-Zip II TFs control ARF10/ARF16 expression, counteracting their negative role on CSC divisions. ATHB2 is induced by auxin in a FEZ-dependent manner, ensuring enhanced proliferation to increasing hormone levels. In the quiescent center (QC), increased ATHB2 expression may promote division to replenish differentiating CSCs, independently of WOX5. In columella cells (CCs), SMB represses FEZ, causing the reduction of HD-Zip II TF levels. In absence of HD-Zip II TFs, the negative action of auxin on proliferation becomes dominant, leading to CC differentiation in concert with SMB. HAT3, which is also expressed in the lower CCs, may contribute to CC differentiation, as inferred from *XVE>HAT3* lines.

starch granules and by spots of cell separation (Fig. S8). A number of hypotheses may help explain context-dependent functions of HD-Zip II TFs in cell fate determination. For example, differences in expression of specific HD-Zip II family members, due to environmental and/or hormonal cues (Ciarbelli et al., 2008; Köllmer et al., 2011; Tan et al., 2018, 2021; Zhang et al., 2014), may shift their relative abundance at the tissue level, thus altering their ability to form homo- or heterodimers with different DNA-binding specificity. Alternatively, tissue-specific differences in chromatin accessibility and/or in the availability of interacting partners may shift HD-Zip II TF activity towards their non-DNA-binding function as transcriptional co-factors (Gallemí et al., 2017; Zheng et al., 2019). All these hypotheses must be taken into account in future research aiming to understand the role of HD-Zip II TFs in the regulation of cell fate determination.

MATERIALS AND METHODS

Plant lines and growth conditions

Wild type used was *Arabidopsis thaliana* (L.) Heynh var. Columbia (Col-0). Insertional *HD-Zip* lines used have been described previously (Turchi et al., 2013): *athb2-2* (gain of function), *hat3-3* (null), *athb2-3* (null), *athb2-1* (null), *athb4-1* (null) and *athb4-3* (null). Multiple *HD-Zip II* mutants used were: *hat3-3 athb4-1*, *hat3-3 athb4-3*, *hat3-2 athb4-1*, *hat3-3 athb2-3*, *athb4-1 athb2-3*, *hat3-3 athb4-1 athb2-1*, *hat3-3 athb4-1 athb2-3*, *hat3-3 athb4-1 athb2-2* and *hat3-3 athb4-1 ATHB2::ATHB2:GUS* (Turchi et al.,

2013). Other lines used were: *pin3-4* (NASC N9363; Friml et al., 2002a), *pin4-3* (NASC N9368; Friml et al., 2002b), *pin7-2* (NASC N9366; Friml et al., 2003), *wox5-1* (Sarkar et al., 2007), *fez-2* (NASC N678269; Willemsen et al., 2008), *smb-3* (NASC N657070; Willemsen et al., 2008) and *arf10-2 arf16-2* (Wang et al., 2005). Marker lines used were: *DR5rev::GFP* (Friml et al., 2003), J2341 (Sabatini et al., 2003), *TAA1::GFP:TAA1* (Stepanova et al., 2008), *HAT3::HAT3:GFP* (Turchi et al., 2013), WOX5::GFP (Sarkar et al., 2007), *FEZ::FEZ:GFP* (Willemsen et al., 2008), pARF10::n3GFP, pARF16::n3GFP (Rademacher et al., 2011), *PIN3::PIN3:GFP*, *PIN4::PIN4:GFP*, *PIN7::PIN7:GFP* (Vieten et al., 2005) and DR5rev::GFP (Friml et al., 2003). Plants were grown vertically on GM medium under light/dark cycles, as previously described (Steindler et al., 1999).

Chemical treatments

To analyze the effect of the chemicals, seedlings were grown for 4 days on GM medium and then transferred on agar plates supplemented with the appropriate drug for 1 day. Concentrations were as follows: DEX, 10µM; NAA, 5 µM (1 µM for ATHB2:GFP experiments). For NAA, β-estradiol and NAA+β-estradiol experiments, plants were grown for 3 days on GM medium then transferred on plates supplemented with 10 µM β-estradiol for 2 days or on 10 µM β-estradiol for 1 day, and further transferred to 10 µM β-estradiol+5 µM NAA for an additional day. For auxinole experiments, seedlings were germinated on control medium or on media supplemented with 5 µM auxinole. Equal amounts of DMSO (ethanol for DEX experiments) were used as the control.

Genetic analysis

The following multiple mutants were generated by crossing: *hat3-3 athb4-1 athb2-3 pin3-4*, *hat3-3 athb4-1 athb2-3 pin4-3*, *hat3-3 athb4-1 athb2-3 pin7-2*, *hat3-3 athb4-1 athb2-3 wox5-1*, *hat3-3 athb4-1 athb2-3 fez-2*, *hat3-3 athb4-1 athb2-3 smb-3* and *hat3-3 athb4-1 athb2-3 arf10 arf16*. All the multiple mutants were selected in F2 by phenotyping and/or PCR genotyping and re-analyzed in F3 (see Table S4 for primer details). Markers J2341, *DR5rev::GFP*, *PIN3::PIN3:GFP*, *PIN4::PIN4:GFP*, *PIN7::PIN7:GFP*, *TAA1::GFP:TAA1* and *WOX5::GFP*, *FEZ::FEZ:GFP* were introduced into *hat3-3 athb4-1 athb2-3* by crossing. *hat3-3 athb4-1 athb2-3* was selected by phenotyping and genotyping. Homozygosity of all the reporters was determined by unanimous GUS and GFP signal ($n \geq 30$).

Gene constructs and transformation

The following DNA constructs were generated: *HAT3::HAT3:YFP*, *ATHB2::ATHB2:GFP*, *ATHB4::ATHB4:GFP*, *35S::HAT3:GR*, *XVE>ATHB4* and *XVE>HAT3*. Primers used to generate all the constructs are listed in Table S4. Col-0, *hat3-3 athb4-1* and *fez-2* plants were transformed as previously described (Steindler et al., 1999). *HAT3::HAT3:YFP* and *ATHB2::ATHB2:GFP* were also introduced in different mutant backgrounds by crossing. Mutant backgrounds were selected by genotyping; homozygosity of the DNA constructs was verified by antibiotic resistance of T3 seedlings.

Phenotypic analysis and statistical methods

Root length and RAM size analyses were carried out on 5- and 10-day-old seedlings, as previously described (Sassi et al., 2012). Lugol's staining was performed on 5-day-old seedlings, as previously described (Willemsen et al., 1998). For differential interference contrast (DIC) microscopy, roots were cleared in chloral hydrate (Weigel and Glazebrook, 2002), mounted on microscope slides and viewed under an Axioskop 2 plus binocular microscope (Zeiss). Images were taken with a Zeiss Axiocam ERc5 s camera. Pairwise statistical comparisons were carried out by means of unpaired *t*-test analysis. For Lugol's analyses, at least 40 samples were analyzed for each genotype and phenotypic distributions were compared using a contingency table followed by Fisher's exact test using GraphPad Quick Calcs.

F-ara-EdU staining

F-ara-EdU staining was carried out as described by Bennett et al.(2014). Four-day-old seedlings were transferred to plates containing 3 µM F-ara-EdU [(2′S)-2′-deoxy-2′-fluoro-5-ethynyluridine] for 1 day and were then fixed in 4% paraformaldehyde. Detection of F-ara-EdU was performed using a Click-iT EdU Alexa Fluor 555 Imaging Kit (Life Technologies) according to the manufacturer's instructions. Seedlings were counterstained with 0.1 µg/ml DAPI (4,6-diamidino-2-phenylindole) and F-ara-EdU incorporation was assessed by confocal microscopy.

Confocal microscopy

Confocal microscopy analyses on roots expressing reporter genes were performed on an Inverted Z.1 microscope equipped with an LSM 700 spectral confocal laser scanning unit (Zeiss). Samples were excited with a 488 nm, 10 mW solid laser with emission at 492-539 nm for green fluorescent protein detection, and with emission at 492-549 nm for yellow fluorescent protein detection. The seedlings were grown for 5 days before imaging. Counterstaining of cell walls was achieved by mounting seedling roots in 10 µM propidium iodide. For F-ara-EdU imaging, excitation was performed using 405 nm and 555 nm lasers; Alexa Fluor 555 fluorescence was detected above 555 nm and DAPI fluorescence below 500 nm. Fluorescence quantitative and semi-quantitative (false-color scale) analyses were carried out using Fiji (https://imagej.net/software/fiji/downloads).

Acknowledgements

With this work, we would like to remember our friend, colleague and woman in science Ida Ruberti, who sadly passed away during the middle stage of this project, for her instrumental role in the conceptualization of the project and the many great discussions of the results. We thank Sabrina Sabatini for providing the J2341 marker line, Ben Scheres for the FEZ::FEZ:GFP line, Xiao-Ya Chen for the *arf10-2 arf16-2* line and Laila Moubayidin for discussions and helpful comments on the manuscript.

Competing interests

The authors declare no competing or financial interests.

Author contributions

Conceptualization: G.M., I.R.; Methodology: M.P., G.S., A.A., L.T., V.R., M.S., G.M., I.R.; Formal analysis: M.P., G.S., A.A., M.S., G.M., I.R.; Investigation: M.P., G.S., A.A., L.T., V.R., M.S.; Data curation: M.P., G.S., M.S., G.M., I.R.; Writing - original draft: M.S., G.M., I.R.; Writing - review & editing: M.P., G.S., M.S., G.M.; Supervision: G.S., M.S., G.M.; Funding acquisition: G.S., G.M., I.R.

Funding

The work was supported by the Ministero delle Politiche Agricole Alimentari e Forestali (BIOTECH Program D. M. 15924 to G.M.), by the Ministero dell'Università e della Ricerca (PRIN 2010HEBBB8_004 to I.R.), by the Regione Lazio POR-FESR 2014-2020 (SMARTBREED project - B85F21003370002) and by the National Center for the Development of New Technologies in Agriculture (Agritech) (European Union Next-Generation EU, PNRR CN00000022 to G.S.).

Data availability

All relevant data can be found within the article and its supplementary information.

Peer review history

The peer review history is available online at https://journals.biologists.com/dev/lookup/doi/10.1242/dev.202586.reviewer-comments.pdf

References

Ai, H., Bellstaedt, J., Bartusch, K. S., Eschen–Lippold, L., Babben, S., Balcke, G. U., Tissier, A., Hause, B., Andersen, T. G., Delker, C. et al. (2023). Auxin–dependent regulation of cell division rates governs root thermomorphogenesis. *EMBO J.* **42**, e111926. doi:10.15252/embj.2022111926

Bennett, T., van den Toorn, A., Willemsen, V. and Scheres, B. (2014). Precise control of plant stem cell activity through parallel regulatory inputs. *Development* **141**, 4055-4064. doi:10.1242/dev.110148

Blilou, I., Xu, J., Wildwater, M., Willemsen, V., Paponov, I., Friml, J., Heidstra, R., Aida, M., Palme, K. and Scheres, B. (2005). The PIN auxin efflux facilitator network controls growth and patterning in Arabidopsis roots. *Nature* **433**, 39-44. doi:10.1038/nature03184

Burkart, R. C., Strotmann, V. I., Kirschner, G. K., Akinci, A., Czempik, L., Dolata, A., Maizel, A., Weidtkamp-Peters, S. and Stahl, Y. (2022). PLETHORA-WOX5 interaction and subnuclear localization control Arabidopsis root stem cell maintenance. *EMBO Rep.* **23**, e54105. doi:10.15252/embr.202154105

Cao, M., Chen, R., Li, P., Yu, Y., Zheng, R., Ge, D., Zheng, W., Wang, X., Gu, Y., Gelová, Z. et al. (2019). TMK1-mediated auxin signalling regulates differential growth of the apical hook. *Nature* **568**, 240-243. doi:10.1038/s41586-019-1069-7

Carabelli, M., Possenti, M., Sessa, G., Ruzza, V., Morelli, G. and Ruberti, I. (2018). Arabidopsis HD-Zip II proteins regulate the exit from proliferation during leaf development in canopy shade. *J. Exp. Bot.* **69**, 5419-5431. doi:10.1093/jxb/ery331

Carabelli, M., Turchi, L., Morelli, G., Østergaard, L., Ruberti, I. and Moubayidin, L. (2021). Coordination of biradial-to-radial symmetry and tissue polarity by HD-ZIP II proteins. *Nat. Commun.* **12**, 4321. doi:10.1038/s41467-021-24550-6

Challa, K. R., Rath, M. and Nath, U. (2019). The CIN-TCP transcription factors promote commitment to differentiation in Arabidopsis leaf pavement cells via both auxin-dependent and independent pathways. *PLoS Genet.* **15**, e1007988. doi:10.1371/journal.pgen.1007988

Ciarbelli, A. R., Ciolfi, A., Salvucci, S., Ruzza, V., Possenti, M., Carabelli, M., Fruscalzo, A., Sessa, G., Morelli, G. and Ruberti, I. (2008). The Arabidopsis homeodomain-leucine zipper II gene family: diversity and redundancy. *Plant Mol. Biol.* **68**, 465-478. doi:10.1007/s11103-008-9383-8

Cruz-Ramírez, A., Díaz-Triviño, S., Wachsman, G., Du, Y., Arteága-Vázquez, M., Zhang, H., Benjamins, R., Blilou, I., Neef, A. B., Chandler, V. et al. (2013). A scarecrow-retinoblastoma protein network controls protective quiescence in the arabidopsis root stem cell organizer. *PLoS Biol.* **11**, e1001724. doi:10.1371/journal.pbio.1001724

Dai, X., Lu, Q., Wang, J., Wang, L., Xiang, F. and Liu, Z. (2021). MiR160 and its target genes ARF10, ARF16 and ARF17 modulate hypocotyl elongation in a light, BRZ, or PAC-dependent manner in Arabidopsis: miR160 promotes hypocotyl elongation. *Plant Sci.* **303**, 110686. doi:10.1016/j.plantsci.2020.110686

De Smet, I. and Beeckman, T. (2011). Asymmetric cell division in land plants and algae: the driving force for differentiation. *Nat. Rev. Mol. Cell Biol.* **12**, 177-188. doi:10.1038/nrm3064

Ding, Z. and Friml, J. (2010). Auxin regulates distal stem cell differentiation in Arabidopsis roots. *Proc. Natl. Acad. Sci. USA* **107**, 12046-12051. doi:10.1073/pnas.1000672107

Dolan, L., Janmaat, K., Willemsen, V., Linstead, P., Poethig, S., Roberts, K. and Scheres, B. (1993). Cellular organisation of the Arabidopsis thaliana root. *Development* **119**, 71-84. doi:10.1242/dev.119.1.71

Dubreuil, C., Jin, X., Grönlund, A. and Fischer, U. (2018). A local auxin gradient regulates root cap self-renewal and size homeostasis. *Curr. Biol.* **28**, 2581-2587. doi:10.1016/j.cub.2018.05.090

Forzani, C., Aichinger, E., Sornay, E., Willemsen, V., Laux, T., Dewitte, W. and Murray, J. A. H. (2014). WOX5 suppresses CYCLIN D activity to establish quiescence at the center of the root stem cell niche. *Curr. Biol.* **24**, 1939-1944. doi:10.1016/j.cub.2014.07.019

Friml, J., Wiśniewska, J., Benková, E., Mendgen, K. and Palme, K. (2002a). Lateral relocation of auxin efflux regulator PIN3 mediates tropism in Arabidopsis. *Nature* **415**, 806-809. doi:10.1038/415806a

Friml, J., Benková, E., Blilou, I., Wisniewska, J., Hamann, T., Ljung, K., Woody, S., Sandberg, G., Scheres, B., Jürgens, G. et al. (2002b). AtPIN4 mediates sink-driven auxin gradients and root patterning in Arabidopsis. *Cell* **108**, 661-673. doi:10.1016/S0092-8674(02)00656-6

Friml, J., Vieten, A., Sauer, M., Weijers, D., Schwarz, H., Hamann, T., Offringa, R. and Jürgens, G. (2003). Efflux-dependent auxin gradients establish the apical-basal axis of Arabidopsis. *Nature* **426**, 147-153. doi:10.1038/nature02085

Gallemí, M., Molina-Contreras, M. J., Paulišić, S., Salla-Martret, M., Sorin, Ç., Godoy, M., Franco-Zorrilla, J. M., Solano, R. and Martínez-Garçia, J. F. (2017). A non-DNA-binding activity for the ATHB4 transcription factor in the control of vegetation proximity. *New Phytol.* **216**, 798-813. doi:10.1111/nph.14727

Hayashi, K.-I., Tan, X., Zheng, N., Hatate, T., Kimura, Y., Kepinski, S. and Nozaki, H. (2008). Small-molecule agonists and antagonists of F-box protein-substrate interactions in auxin perception and signaling. *Proc. Natl. Acad. Sci. USA* **105**, 5632-5637. doi:10.1073/pnas.0711146105

Hayashi, K. I., Neve, J., Hirose, M., Kuboki, A., Shimada, Y., Kepinski, S. and Nozaki, H. (2012). Rational design of an auxin antagonist of the SCF TIR1 auxin receptor complex. *ACS Chem. Biol.* **7**, 590-598. doi:10.1021/cb200404c

He, G., Liu, P., Zhao, H. and Sun, J. (2020). The HD-ZIP II transcription factors regulate plant architecture through the auxin pathway. *Int. J. Mol. Sci.* **21**, 3250. doi:10.3390/ijms21093250

Heyman, J., Cools, T., Vandenbussche, F., Heyndrickx, K. S., Van Leene, J., Vercauteren, I., Vanderauwera, S., Vandepoele, K., De Jaeger, G., Van Der Straeten, D. et al. (2013). ERF115 controls root quiescent center cell division and stem cell replenishment. *Science* **342**, 860-863. doi:10.1126/science.1240667

Hong, J. H., Chu, H., Zhang, C., Ghosh, D., Gong, X. and Xu, J. (2015). A quantitative analysis of stem cell homeostasis in the arabidopsis columella root cap. *Front. Plant Sci.* **6**, 206. doi:10.3389/fpls.2015.00206

Hong, J. H., Savina, M., Du, J., Devendran, A., Kannivadi Ramakanth, K., Tian, X., Sim, W. S., Mironova, V. V. and Xu, J. (2017). A sacrifice-for-survival mechanism protects root stem cell niche from chilling stress. *Cell* **170**, 102-113.e14. doi:10.1016/j.cell.2017.06.002

Köllmer, I., Werner, T. and Schmülling, T. (2011). Ectopic expression of different cytokinin-regulated transcription factor genes of Arabidopsis thaliana alters plant growth and development. *J. Plant Physiol.* **168**, 1320-1327. doi:10.1016/j.jplph.2011.02.006

Liu, Y. and von Wirén, N. (2022). Integration of nutrient and water availabilities via auxin into the root developmental program. *Curr. Opin. Plant Biol.* **65**, 102117. doi:10.1016/j.pbi.2021.102117

Lv, B., Yu, Q., Liu, J., Wen, X., Yan, Z., Hu, K., Li, H., Kong, X., Li, C., Tian, H. et al. (2020). Non-canonical AUX/IAA protein IAA33 competes with canonical AUX/IAA repressor IAA5 to negatively regulate auxin signaling. *EMBO J.* **39**, e101515. doi:10.15252/embj.2019101515

Marhava, P., Hoermayer, L., Yoshida, S., Marhavy′, P., Benková, E. and Friml, J. (2019). Re-activation of stem cell pathways for pattern restoration in plant wound healing. *Cell* **177**, 957-969. doi:10.1016/j.cell.2019.04.015

Merelo, P., Ram, H., Caggiano, M. P., Ohno, C., Ott, F., Straub, D., Graeff, M., Cho, S. K., Yang, S. W., Wenkel, S. et al. (2016). Regulation of MIR165/166 by class II and class III homeodomain leucine zipper proteins establishes leaf polarity. *Proc. Natl. Acad. Sci. USA* **113**, 11973-11978. doi:10.1073/pnas.1516110113

Mutte, S. K., Kato, H., Rothfels, C., Melkonian, M., Wong, G. K. S. and Weijers, D. (2018). Origin and evolution of the nuclear auxin response system. *Elife* **7**, e33399. doi:10.7554/eLife.33399

Pardal, R. and Heidstra, R. (2021). Root stem cell niche networks: it's complexed! Insights from Arabidopsis. *J. Exp. Bot.* **72**, 6727-6738. doi:10.1093/jxb/erab272

Pi, L., Aichinger, E., van der Graaff, E., Llavata-Peris, C. I., Weijers, D., Hennig, L., Groot, E. and Laux, T. (2015). Organizer-derived WOX5 signal maintains root columella stem cells through chromatin-mediated repression of CDF4 expression. *Dev. Cell* **33**, 576-588. doi:10.1016/j.devcel.2015.04.024

Pierre-Jerome, E., Drapek, C. and Benfey, P. N. (2018). Regulation of division and differentiation of plant stem cells. *Annu. Rev. Cell Dev. Biol.* **34**, 289-310. doi:10.1146/annurev-cellbio-100617-062459

Pillitteri, L. J., Guo, X. and Dong, J. (2016). Asymmetric cell division in plants: mechanisms of symmetry breaking and cell fate determination. *Cell. Mol. Life Sci.* **73**, 4213-4229. doi:10.1007/s00018-016-2290-2

Rademacher, E. H., Möller, B., Lokerse, A. S., Llavata-Peris, C. I., van den Berg, W. and Weijers, D. (2011). A cellular expression map of the Arabidopsis AUXIN RESPONSE FACTOR gene family. *Plant J.* **68**, 597-606. doi:10.1111/j.1365-313X.2011.04710.x

Ruberti, I., Sessa, G., Ciolfi, A., Possenti, M., Carabelli, M. and Morelli, G. (2012). Plant adaptation to dynamically changing environment: the shade avoidance response. *Biotechnol. Adv.* **30**, 1047-1058. doi:10.1016/j.biotechadv.2011.08.014

Sabatini, S., Beis, D., Wolkenfelt, H., Murfett, J., Guilfoyle, T., Malamy, J., Benfey, P., Leyser, O., Bechtold, N., Weisbeek, P. et al. (1999). An auxin-dependent distal organizer of pattern and polarity in the Arabidopsis root. *Cell* **99**, 463-472. doi:10.1016/S0092-8674(00)81535-4

Sabatini, S., Heidstra, R., Wildwater, M. and Scheres, B. (2003). SCARECROW is involved in positioning the stem cell niche in the Arabidopsis root meristem. *Genes Dev.* **17**, 354-358. doi:10.1101/gad.252503

Sarkar, A. K., Luijten, M., Miyashima, S., Lenhard, M., Hashimoto, T., Nakajima, K., Scheres, B., Heidstra, R. and Laux, T. (2007). Conserved factors regulate signalling in Arabidopsis thaliana shoot and root stem cell organizers. *Nature* **446**, 811-814. doi:10.1038/nature05703

Sassi, M., Lu, Y., Zhang, Y., Wang, J., Dhonukshe, P., Blilou, I., Dai, M., Li, J., Gong, X., Jaillais, Y. et al. (2012). COP1 mediates the coordination of root and shoot growth by light through modulation of PIN1- and PIN2-dependent auxin transport in Arabidopsis. *Development* **139**, 3402-3412. doi:10.1242/dev.078212

Savina, M. S., Pasternak, T., Omelyanchuk, N. A., Novikova, D. D., Palme, K., Mironova, V. V. and Lavrekha, V. V. (2020). Cell dynamics in WOX5-overexpressing root tips: the impact of local auxin biosynthesis. *Front. Plant Sci.* **11**, 560169. doi:10.3389/fpls.2020.560169

Sawa, S., Ohgishi, M., Goda, H., Higuchi, K., Shimada, Y., Yoshida, S. and Koshiba, T. (2002). The HAT2 gene, a member of the HD-Zip gene family, isolated as an auxin inducible gene by DNA microarray screening, affects auxin response in Arabidopsis. *Plant J.* **32**, 1011-1022. doi:10.1046/j.1365-313X.2002.01488.x

Scheres, B. (2007). Stem-cell niches: nursery rhymes across kingdoms. *Nat. Rev. Mol. Cell Biol.* **8**, 345-354. doi:10.1038/nrm2164

Sessa, G., Carabelli, M., Possenti, M., Morelli, G. and Ruberti, I. (2018). Multiple pathways in the control of the shade avoidance response. *Plants* **7**, 102. doi:10.3390/plants7040102

Shimotohno, A. and Scheres, B. (2019). Topology of regulatory networks that guide plant meristem activity: similarities and differences. *Curr. Opin. Plant Biol.* **51**, 74-80. doi:10.1016/j.pbi.2019.04.006

Steindler, C., Matteucci, A., Sessa, G., Weimar, T., Ohgishi, M., Aoyama, T., Morelli, G. and Ruberti, I. (1999). Shade avoidance responses are mediated by the ATHB-2 HD-zip protein, a negative regulator of gene expression. *Development* **126**, 4235-4245. doi:10.1242/dev.126.19.4235

Stepanova, A. N., Robertson-Hoyt, J., Yun, J., Benavente, L. M., Xie, D.-Y., Dolezal, K., Schlereth, A., Jürgens, G. and Alonso, J. M. (2008). TAA1-mediated auxin biosynthesis is essential for hormone crosstalk and plant development. *Cell* **133**, 177-191. doi:10.1016/j.cell.2008.01.047

Tan, W., Zhang, D., Zhou, H., Zheng, T., Yin, Y. and Lin, H. (2018). Transcription factor HAT1 is a substrate of SnRK2.3 kinase and negatively regulates ABA

synthesis and signaling in Arabidopsis responding to drought. *PLoS Genet.* **14**, e1007336. doi:10.1371/journal.pgen.1007336

Tan, W., Han, Q., Li, Y., Yang, F., Li, J., Li, P., Xu, X., Lin, H. and Zhang, D. (2021). A HAT1-DELLA signaling module regulates Trichome initiation and leaf growth by achieving gibberellin homeostasis. *New Phytol.* **231**, 1220-1235. doi:10.1111/nph.17422

Tian, H., Wabnik, K., Niu, T., Li, H., Yu, Q., Pollmann, S., Vanneste, S., Govaerts, W., Rolčík, J., Geisler, M. et al. (2014). WOX5-IAA17 feedback circuit-mediated cellular auxin response is crucial for the patterning of root stem cell niches in Arabidopsis. *Mol. Plant* **7**, 277-289. doi:10.1093/mp/sst118

Truskina, J., Han, J., Chrysanthou, E., Galvan-Ampudia, C. S., Lainé, S., Brunoud, G., Macé, J., Bellows, S., Legrand, J., Bågman, A. M. et al. (2021). A network of transcriptional repressors modulates auxin responses. *Nature* **589**, 116-119. doi:10.1038/s41586-020-2940-2

Turchi, L., Carabelli, M., Ruzza, V., Possenti, M., Sassi, M., Peñalosa, A., Sessa, G., Salvi, S., Forte, V., Morelli, G. et al. (2013). Arabidopsis HD-Zip II transcription factors control apical embryo development and meristem function. *Development* **140**, 2118-2129. doi:10.1242/dev.092833

Vieten, A., Vanneste, S., Wisniewska, J., Benková, E., Benjamins, R., Beeckman, T., Luschnig, C. and Friml, J. (2005). Functional redundancy of PIN proteins is accompanied by auxin-dependent cross-regulation of PIN expression. *Development* **132**, 4521-4531. doi:10.1242/dev.02027

Wanamaker, S. A., Garza, R. M., MacWilliams, A., Nery, J. R., Bartlett, A., Castanon, R., Goubil, A., Feeney, J., O'Malley, R., Huang, S. C. et al. (2017). CrY2H-seq: a massively multiplexed assay for deep-coverage interactome mapping. *Nat. Methods* **14**, 819-825. doi:10.1038/nmeth.4343

Wang, J. W., Wang, L. J., Mao, Y. B., Cai, W. J., Xue, H. W. and Chen, X. Y. (2005). Control of root cap formation by MicroRNA-targeted auxin response factors in Arabidopsis. *Plant Cell* **17**, 2204-2216. doi:10.1105/tpc.105.033076

Wang, J., Li, X., Chen, X., Tang, W., Yu, Z., Xu, T., Tian, H. and Ding, Z. (2023). Dual regulations of cell cycle regulator DPa by auxin in Arabidopsis root distal stem cell maintenance. *Proc. Natl. Acad. Sci. USA* **120**, e2218503120. doi:10.1073/pnas.2218503120

Weigel, D. and Glazebrook, J. (2002). *Arabidopsis: A Laboratory Manual*. CSHL Press.

Weijers, D., Schlereth, A., Ehrismann, J. S., Schwank, G., Kientz, M. and Jürgens, G. (2006). Auxin triggers transient local signaling for cell specification in Arabidopsis embryogenesis. *Dev. Cell* **10**, 265-270. doi:10.1016/j.devcel.2005.12.001

Willemsen, V., Wolkenfelt, H., de Vrieze, G., Weisbeek, P. and Scheres, B. (1998). The HOBBIT gene is required for formation of the root meristem in the Arabidopsis embryo. *Development* **125**, 521-531. doi:10.1242/dev.125.3.521

Willemsen, V., Bauch, M., Bennett, T., Campilho, A., Wolkenfelt, H., Xu, J., Haseloff, J. and Scheres, B. (2008). The NAC domain transcription factors FEZ and SOMBRERO control the orientation of cell division plane in Arabidopsis root stem cells. *Dev. Cell* **15**, 913-922. doi:10.1016/j.devcel.2008.09.019

Yuan, T. T., Xiang, Z. X., Li, W., Gao, X. and Lu, Y. T. (2021). Osmotic stress represses root growth by modulating the transcriptional regulation of PIN-FORMED3. *New Phytol.* **232**, 1661-1673. doi:10.1111/nph.17687

Zhang, D., Ye, H., Guo, H., Johnson, A., Zhang, M., Lin, H. and Yin, Y. (2014). Transcription factor HAT1 is phosphorylated by BIN2 kinase and mediates brassinosteroid repressed gene expression in Arabidopsis. *Plant J.* **77**, 59-70. doi:10.1111/tpj.12368

Zheng, T., Tan, W., Yang, H., Li, T., Liu, B., Zhang, D. and Lin, H. and Lin, H. (2019). Regulation of anthocyanin accumulation via MYB75/HAT1/TPL-mediated transcriptional repression. *PLoS Genet.* **15**, e1007993. doi:10.1371/journal.pgen.1007993